The Embryonic Vertebrate Heart Tube Is a Dynamic Suction Pump

Arian S. Forouhar, *et al.*

Science **312**, 751 (2006);
DOI: 10.1126/science.1123775

different tudor domains (Fig. 4B), perhaps reflecting the structural flexibility needed for accommodating different binding partners.

Because of the involvement in transcription regulation, it is tempting to speculate that the double tudor domain is responsible for directing JMJD2A to chromatin regions enriched with H3-K4 or H4-K20 methylation. However, alternative scenarios are also possible, and the functional relation between methyl-histone binding by the double tudor domain and histone demethylation by JMJD2A in a physiological context remains to be established. Nevertheless, our results demonstrate that the hybrid-tudor domain structure of JMJD2A is required for the formation of a functional methyl-histone H3 binding module. The unusual fold requires two tudor domain motifs in tandem, which is only present in a subset of tudor domain–containing proteins including JMJD2 family members and 53BP1. It will be extremely interesting to understand the principle underlying the distinct folding of the double tudor domains of JMJD2A and 53BP1 despite their sequence similarity. Many chromatin-associated proteins have closely spaced tandem repeats of effector domains implicated in histone binding, including the bromo, chromo, MBT, Agenet, and tudor domains. Our discovery reveals the potential for forming novel histone binding modules from the familiar effector domains.

References and Notes

1. T. Jenuwein, C. D. Allis, *Science* **293**, 1074 (2001).
2. C. Martin, Y. Zhang, *Nat. Rev. Mol. Cell Biol.* **6**, 838 (2005).
3. C. Dhalluin *et al.*, *Nature* **399**, 491 (1999).
4. R. H. Jacobson, A. G. Ladurner, D. S. King, R. Tjian, *Science* **288**, 1422 (2000).
5. S. A. Jacobs, S. Khorasanizadeh, *Science* **295**, 2080 (2002).
6. P. R. Nielsen *et al.*, *Nature* **416**, 103 (2002).
7. J. Min, Y. Zhang, R. M. Xu, *Genes Dev.* **17**, 1823 (2003).
8. W. Fischle *et al.*, *Genes Dev.* **17**, 1870 (2003).
9. J. F. Flanagan *et al.*, *Nature* **438**, 1181 (2005).
10. J. Wysocka *et al.*, *Cell* **121**, 859 (2005).
11. S. Maurer-Stroh *et al.*, *Trends Biochem. Sci.* **28**, 69 (2003).
12. J. Kim *et al.*, *EMBO Rep.* **7**, 397 (2006).
13. Y.-i. Tsukada *et al.*, *Nature* **439**, 811 (2006).
14. D. Zhang, H. G. Yoon, J. Wong, *Mol. Cell. Biol.* **25**, 6404 (2005).
15. S. G. Gray *et al.*, *J. Biol. Chem.* **280**, 28507 (2005).
16. R. Sprangers, M. R. Groves, I. Sinning, M. Sattler, *J. Mol. Biol.* **327**, 507 (2003).
17. Y. Huyen *et al.*, *Nature* **432**, 406 (2004).
18. G. Charier *et al.*, *Structure* **12**, 1551 (2004).

19. We thank D. Schneider and A. Heroux for help at the X26C beamline of the National Synchrotron Light Source (Brookhaven National Laboratory), and L. Henry and S. Shaw for comments on the manuscript. The coordinates and the structure factors have been deposited with the RCSB (Research Collaboratory for Structural Bioinformatics) Protein Data Bank with accession codes 2GFA (H3K4Me3 bound) and 2GF7 (free). The work was supported in part by the W. M. Keck foundation (R.-M.X.), the Howard Hughes Medical Institute (Y.Z.), and NIH grants GM 63718 (R.M.X.), GM68804 (Y.Z.), and DK62248 (M.T.B.). Y.Z. is an Investigator of the Howard Hughes Medical Institute.

Supporting Online Material

www.sciencemag.org/cgi/content/full/1125162/DC1
Materials and Methods
Fig. S1
Table S1
References

19 January 2006; accepted 27 March 2006
Published online 6 April 2006;
10.1126/science.1125162
Include this information when citing this paper.

The Embryonic Vertebrate Heart Tube Is a Dynamic Suction Pump

Arian S. Forouhar,[1] Michael Liebling,[2] Anna Hickerson,[1] Abbas Nasiraei-Moghaddam,[1] Huai-Jen Tsai,[4] Jay R. Hove,[5] Scott E. Fraser,[1,2] Mary E. Dickinson,[2,6] Morteza Gharib[1,3]*

The embryonic vertebrate heart begins pumping blood long before the development of discernable chambers and valves. At these early stages, the heart tube has been described as a peristaltic pump. Recent advances in confocal laser scanning microscopy and four-dimensional visualization have warranted another look at early cardiac structure and function. We examined the movement of cells in the embryonic zebrafish heart tube and the flow of blood through the heart and obtained results that contradict peristalsis as a pumping mechanism in the embryonic heart. We propose a more likely explanation of early cardiac dynamics in which the pumping action results from suction due to elastic wave propagation in the heart tube.

The cardiovascular system is the first functional organ system to develop in vertebrate embryos. In its earliest stages, it consists of a primitive heart tube that drives blood through a simple vascular network. Cardiac physiologists have long conjectured that the valveless embryonic heart tube drives circulation by means of peristaltic contractions (*1*, *2*), a pumping mechanism that pushes blood through the heart tube by progressively reducing the tube volume (*3*). Confirmation of this pumping mechanism requires in vivo visualization and quantification of both heart wall motion and blood cell motion, which are difficult with traditional imaging modalities. The zebrafish offers a powerful vertebrate model for cardiogenetic studies (*4*–*7*) with multiple advantages for in vivo imaging: Eggs are externally fertilized; embryos are nearly transparent, providing optical access to the earliest stages of cardiogenesis; and many GFP (green fluorescent protein)-labeled transgenic strains have been derived.

Recent improvements in confocal microscopy and four-dimensional (three spatial dimensions plus time) reconstruction protocols (*8*) permit us to take full advantage of these qualities and revisit the pumping mechanism of the early embryonic heart tube. We tested three implications of peristaltic pumping in the heart, namely that (i) there should be a unidirectional wave traveling along the endocardial layer, (ii) blood cell velocities should be bounded in magnitude by the instantaneous traveling wave speed through the heart tube wall, and (iii) cardiac output should increase linearly with heart rate.

To test the nature of cardiac pumping, we used in vivo high-speed confocal imaging of zebrafish hearts before valve formation. Optical sections through 26–hours postfertilization (hpf) *Tg(gata1:GFP)* zebrafish hearts expressing GFP in blood cells, endocardium, and myocardium were reconstructed into four-dimensional data sets (*8*) (Fig. 1A and movie S1), which provided direct three-dimensional data on the position of myocardial and endocardial cells throughout the cardiac cycle (Figs. 1B and 2 and movies S1 to S3). By tracking the position of the trailing edge of the endocardial wave crest during the cardiac cycle, we identified the speed and the direction of the traveling wave through the heart wall. The wave originates in myocardial cells positioned near the inflow tract of the heart tube (Fig. 2), and upon contraction a bidirectional wave propagates axially along the heart tube wall (Fig. 1 and movies S1 and S2). The proximity of the pacemaker cells to the venous boundary of the heart tube, along with the speed of the traveling wave, combine to make this bidirectional wave undetectable through traditional imaging modalities.

In a peristaltic heart tube model, the net flow is exactly equal to the volume displaced during contractions. This dynamic imposes a direct relationship between the upstream blood velocity and the local traveling wave velocity. Specifically, because peristalsis is governed by static pressure rather than dynamic pressure (*3*),

[1]Option in Bioengineering, [2]Biological Imaging Center, Beckman Institute, [3]Graduate Aeronautical Laboratories, California Institute of Technology (Caltech), Pasadena, CA 91125, USA. [4]Institute of Molecular and Cellular Biology, National Taiwan University, Taiwan. [5]Genome Research Institute, University of Cincinnati, Cincinnati, OH 45221, USA. [6]Department of Molecular Physiology and Biophysics, Baylor College of Medicine, Houston, TX 77030, USA.

*To whom correspondence should be addressed. E-mail: mgharib@caltech.edu

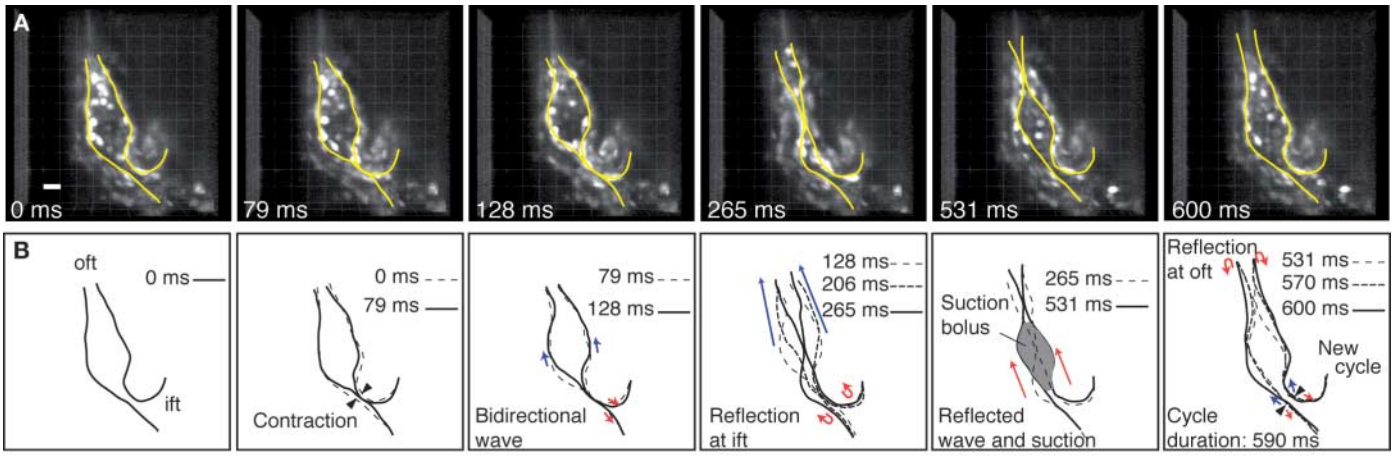

Fig. 1. Biomechanics of embryonic heart tube contractions contradicts peristalsis as the main pumping mechanism. (**A**) Three-dimensional reconstructions of a 26-hpf *Tg(gata1:GFP)* zebrafish heart tube at six time points. Yellow lines denote the shape of the endocardial layer. (**B**) Superimposed outlines of different time points highlight bidirectional traveling wave (red and blue arrows). Black arrowheads indicate contraction location. Shaded gray region indicates suction bolus. Regions of mismatched impedance at the inflow tract (ift) and outflow tract (oft) of the heart tube are reflection sites. Grid spacing is 20 μm.

it would imply that the upstream blood velocity in the zebrafish heart does not exceed the simultaneous local traveling wave velocity. However, in each of the cases observed (n = 5), the maximum velocity of the upstream blood accelerated to velocities exceeding the wall wave speed (Fig. 3, A to C).

To investigate how the cardiac output varied with the contractile wave frequency in vivo, we altered temperature to manipulate heart rates and tracked blood cells to determine flow rates. In this temperature range (24°C to 34°C), fish develop normally, and we do not expect a nonlinear change in blood viscosity. If the heart tube were a peristaltic pump, the cardiac output should increase linearly with the contractile wave frequency. However, we found that the blood velocity response, and thus the net flow rate response, to a monotonic heart rate change is nonlinear (Fig. 3D).

These three observations indicate that the embryonic heart tube does not act as a peristaltic pump; instead, they seem consistent with a previously investigated hydro-impedance pump model (*9*). In this model of valveless pumping, the pumping action results from elastic wave propagation and reflection in the heart tube; resonance conditions arise at certain frequencies where the phase speed permits constructive interference between the incident and reflected pressure waves. Mechanical properties of the system such as diameter, length, elasticity, and pressure dictate wave speed as well as attenuation and reflection coefficients in the system. The impedance pump model exhibits a sensitivity of the generated flow to the activation frequency that is similar in many ways to our in vivo observations (Fig. 3D), including nonlinear flow with frequency, domains of negative slope, and resonance frequencies that allow higher flow rates than peristalsis.

The impedance pump model requires mismatches in impedance to induce wave reflections at the boundaries of the pump element and to build up suction and induce net flow (*9*). In zebrafish, many mechanical properties of the heart tube boundaries contribute to mismatched impedance. The most prominent feature at the inflow boundary of the heart tube is a drastic change in diameter (Fig. 4, A and B). The heart tube stems from the surface of the spherical yolk sac, acutely narrows to about 30 μm, and becomes lined by an additional layer of cells (myocardium) and cardiac jelly that alters the elasticity of the heart tube at the inflow boundary (Fig. 4, A and B). Our four-dimensional data confirmed that this region of mismatch impedance is indeed a site of wave reflections. Pacemaker cell contractions initiate axial waves that travel along the heart tube until they reach the heart tube boundaries. When these waves reach the inflow and outflow boundaries, they reflect in the form of sudden expansions and begin to travel back through the heart tube (movies S1 and S2).

The sudden expansions of the cardiac lumen at the reflection sites create low-pressure zones and suck blood through the heart tube (movie S1). In order to describe this suction mechanism in vivo, we looked at the pressure-flow relationship through the heart tube during the

Fig. 2. Heart tube contractions convey active and passive regions. (**A**) Three-dimensional reconstruction of a 26-hpf *Tg(cmlc2:GFP)* embryo. Myocytes are fluorescently labeled, and their three-dimensional trajectories during two complete cardiac cycles are shown. The red double-arrow line indicates the active pacemaker region and the double-arrow white line, the passive region. The orthogonal scale bar triplet indicates 20 μm in each direction. (**B**) The active pacemaker region spans the first 20 μm of the heart tube. It was identified by calculating the time difference between the moment myocardial cells at a given position along the tube experience a 10 to 13% strain rate with neighboring cells and the time at which they each reach 90% of their maximal displacement. When this time difference is nearly zero, the region experiences active contraction.

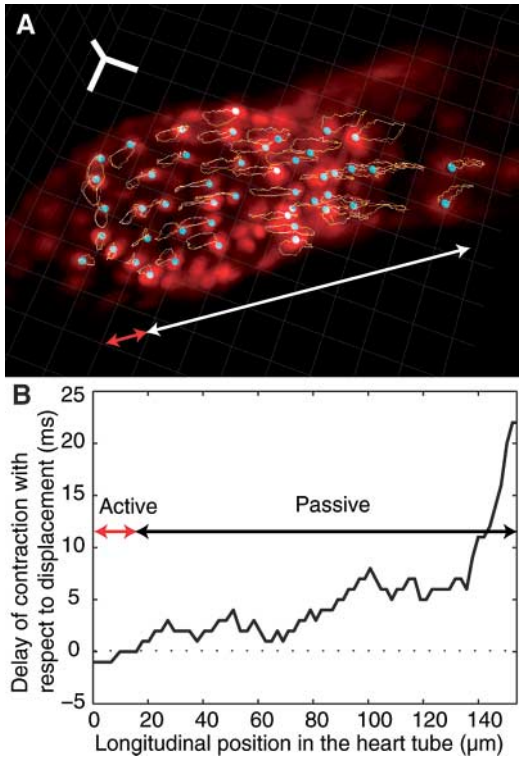

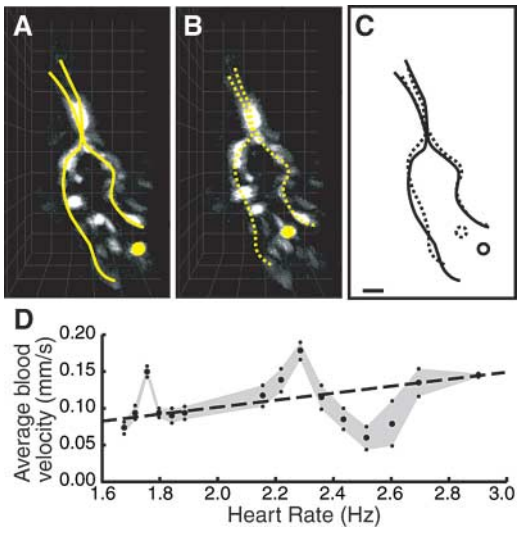

Fig. 3. Blood cell motions demonstrate nonperistaltic pumping mechanism in the embryonic heart tube. (**A** and **B**) Reconstruction of a 26-hpf Tg(*gata1*::GFP) embryo. The endocardial layer, along with a blood cell, have been marked in yellow in each image. (**C**) Superposition of schematics in (A) and (B). Blood cell displacement is much greater than traveling wave crest displacement, indicating that blood cells do not passively follow the traveling wave. Scale bar indicates 20 μm. (**D**) Nonlinear frequency-flow relationship for 26-hpf zebrafish heart tube (Materials and Methods). Resonance peaks in the observed average blood velocity at 1.75 and 2.3 Hz exceed the expected estimate for peristaltic pumping (dashed line).

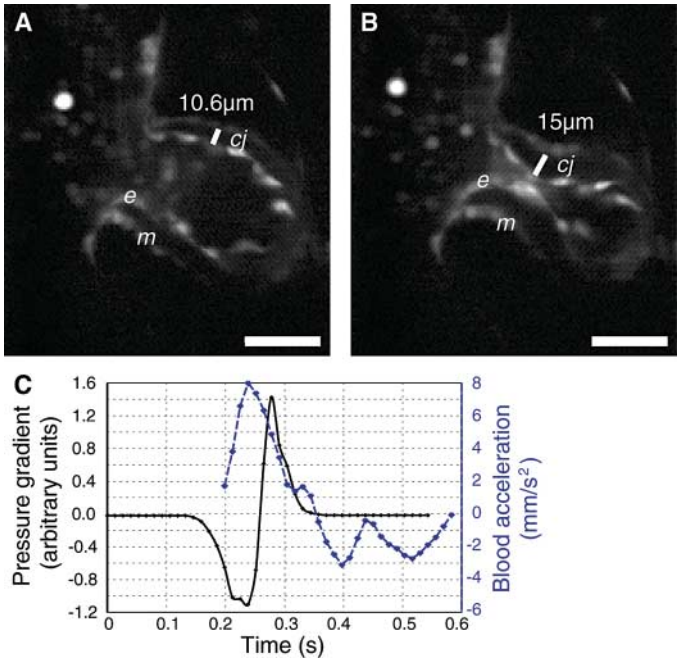

Fig. 4. Hydroelastic-based suction mechanism in the embryonic heart tube. (**A**) Inflow region of a 26-hpf embryo. The distance between the myocardial (m) and endocardial (e) layers is marked (short diagonal white bars). (**B**) Upon contraction, this distance increases. The expansion of the cardiac jelly (cj) at the site of contraction illustrates the elastic nature of the heart wall, a requirement of the impedance pump model. This observation contradicts the muscularly driven peristaltic mechanism because the concentric rings of endocardium and myocardium do not approach each other during contraction. Scale bars, 50 μm. (**C**) Blood cell accelerations and estimated pressure gradient as a function of time (Materials and Methods). The maximum acceleration occurs when the pressure gradient is negative, indicating that the embryonic heart tube acts as a suction pump.

cardiac cycle. By measuring the radius of the cardiac lumen at two cross sections a short distance apart, we deduced the pressure gradient at a point (*10*) (Fig. 4C and movie S4). In this region, blood cells first begin to accelerate when the pressure gradient is negative, analogous to drinking liquid through a straw. Blood cells continue to accelerate, reaching a maximum as the pressure gradient climbs from negative values toward zero. As the pressure gradient continues to increase from zero to positive values, blood cells continue to move forward but with decreasing accelerations. Lastly, when the pressure gradient reaches a maximum and begins to decrease, blood cells decelerate until they finally reach a resting point. Importantly, a phase difference between the maximum acceleration and the maximum pressure gradient exists. Specifically, blood reaches a maximum acceleration a short time after there is a local minimum in the pressure gradient. This time lag between suction pressure and flow in the embryonic heart resembles the pressure-flow relationship of a fluid dynamic pump (*3*) rather than a peristaltic mechanism, where such a time lag should not exist.

By using new in vivo imaging tools, we have taken a closer look at early cardiac structure and function and identified three biomechanical properties of embryonic heart tube contractions that contradict cardiac peristalsis: (i) a bidirectional, as opposed to unidirectional, wave traverses the endocardial layer, (ii) blood cell trajectories do not follow local endocardial wave trajectories and exhibit velocities greater than those of the traveling wave, and (iii) the frequency-flow relationship is nonlinear and exceeds the maximum flow rate possible for a peristaltic pump. Furthermore, we observed (i) resonance peaks in the frequency-flow relationship; (ii) mismatched impedance at inflow and outflow tracts and visible wave reflections at the heart tube boundaries; and (iii) a pressure-flow relationship that exhibits a phase difference between the maximum acceleration of blood and the maximum local pressure gradient. Thus, the valveless embryonic heart does not drive circulation through peristalsis. Instead, these observations suggest a hydroelastic impedance pump model based on elastic wave propagation and reflection (*9*). The simple mechanism we propose requires only a single actuation site rather than complete synchrony throughout the heart tube. The frequency-dependent sensitivity of this pumping mechanism itself suggests that such valveless pumping may not be suitable for postembryonic circulation in ectotherms. The presented characterization of early cardiac biomechanics should provide the foundation to revisit many aspects of embryonic cardiogenesis and provides evidence for an embryonic root to the observed suction action of the adult heart (*11*).

References and Notes

1. M. C. Fishman, K. R. Chien, *Development* **124**, 2099 (1997).
2. S. F. Gilbert, *Developmental Biology* (Sinauer, Sunderland, MA, 2000).
3. S. Vogel, *Life in Moving Fluids* (Princeton Univ. Press, Princeton, NJ, 1994), pp. 323–329.
4. M. Fishman, *Science* **294**, 1290 (2001).
5. J. R. Hove *et al.*, *Nature* **421**, 172 (2003).
6. D. Y. Stainier, *Nat. Rev. Genet.* **2**, 39 (2001).
7. D. Yelon, *Dev. Dyn.* **222**, 552 (2001).
8. M. Liebling, A. S. Forouhar, M. Gharib, S. E. Fraser, M. E. Dickinson, *J. Biomed. Opt.* **10**, 054001 (2005).
9. A. I. Hickerson, D. Rinderknecht, M. Gharib, *Exp. Fluids* **38**, 534 (2005).
10. W. W. Nichols, M. F. O'Rourke, *McDonald's Blood Flow in Arteries* (Oxford Univ. Press, New York, 1988), pp. 98–102.
11. G. D. Buckberg *et al.*, *Semin. Thorac. Cardiovasc. Surg.* **13**, 342 (2001).
12. We thank J. Dabiri, M. Milano, J. Vermot, and J. Pierce for comments on the paper; S. Megason and L. Trinh for help with zebrafish and imaging techniques; and S. Lin for providing the *Tg(gata1:GFP)* zebrafish line. This work was supported by American Heart Association grant 03665071Y (J.R.H.), NIH grant 5R01HL078694 (S.E.F., M.E.D., and M.L.), and Swiss National Science Foundation grants PBEL2-104418 and PA002-111433 (M.L.).

Supporting Online Material

www.sciencemag.org/cgi/content/full/312/5774/751/DC1
Materials and Methods
Figs. S1 and S2
Movies S1 to S4

13 December 2005; accepted 6 April 2006
10.1126/science.1123775